Hindawi Publishing Corporation
Mathematical Problems in Engineering
Volume 2016, Article ID 3436192, 11 pages
http://dx.doi.org/10.1155/2016/3436192

Research Article

Using EVT for Geological Anomaly Design and Its Application in Identifying Anomalies in Mining Areas

Feilong Qin,[1] Bingli Liu,[1,2] and Ke Guo[1]

[1]*Chengdu University of Technology, The Key Laboratory of Mathematical Geology in Sichuan, Chengdu 610059, China*
[2]*Institute of Geophysical and Geochemical Exploration, Chinese Academy of Geoscience, Langfang 065000, China*

Correspondence should be addressed to Bingli Liu; liubingli-82@163.com

Received 28 April 2016; Revised 21 July 2016; Accepted 21 August 2016

Academic Editor: Cheng-Tang Wu

A geological anomaly is the basis of mineral deposit prediction. Through the study of the knowledge and characteristics of geological anomalies, the category of extreme value theory (EVT) to which a geological anomaly belongs can be determined. Associating the principle of the EVT and ensuring the methods of the shape parameter and scale parameter for the generalized Pareto distribution (GPD), the methods to select the threshold of the GPD can be studied. This paper designs a new algorithm called the EVT model of geological anomaly. These study data on Cu and Au originate from 26 exploration lines of the Jiguanzui Cu-Au mining area in Hubei, China. The proposed EVT model of the geological anomaly is applied to identify anomalies in the Jiguanzui Cu-Au mining area. The results show that the model can effectively identify the geological anomaly region of Cu and Au. The anomaly region of Cu and Au is consistent with the range of ore bodies of actual engineering exploration. Therefore, the EVT model of the geological anomaly can effectively identify anomalies, and it has a high indicating function with respect to ore prospecting.

1. Introduction

In mineral deposit prediction, searching for mineral deposits requires identification of a geological anomaly indicating that the economic value is high ("as discussed by Darehshiri et al. [1]"). A geological anomaly is a geological body or complex of bodies with obvious different compositions, structures, or orders of genesis as compared with the surrounding circumstances ("as discussed by Lu and Zhao [2]"). With the evolution of the earth, the nature, source, and intensity of force will not be the same across different times and space. In addition, the distribution of material of the earth is not uniform in time and space, which results in different events and responses, such as the tension and compression of layers, deposition and erosion of material, subsidence and uplift of the crust, simple and complex structures, and intrusion and ejection of magma; these differences form the geological anomaly ("as discussed by Pengda et al. [3]"). If a numerical value or numerical interval is used as a threshold to represent the background field, the field that is above or below the threshold constitutes a geological anomaly ("as discussed by Cheng [4]"). The character of the geological anomaly and the size and type of mineral resources are determined by the geological environment, geological age, rock type, and structural background of the formation of the geological anomaly. With the evolution of geology, the geological anomaly has an evolution sequence in the time and space. With respect to time, evolution has the stage; with respect to space, evolution has inheritance and superposition ("as discussed by Freedman and Parsons [5]").

Not all geological anomalies can form deposits, but the constitution of a geological anomaly is a prerequisite for the formation of deposits ("as discussed by Shen et al. [6]"). Determining which geological anomaly can result in a mineral deposit can allow effective identification of the deposit. Based on the time required for ore formation, a geological anomaly can be classified into a front ore-forming anomaly, an ore-forming anomaly, and a tail ore-forming anomaly ("as discussed by Zhao et al. [7]"). Different factors and combinations of ore-forming geologies have certain special properties related to ore formation. However, various minerals with different genetic, morphological, mineral, and

industrial types are needed to select certain geological factors and combinations. Therefore, it is necessary to find the target anomaly in all of the possible ore-forming geological anomalies; the area of the target anomaly is known as the feasible location for prospecting. According to additional information on ore formation, such as the remote sensing anomaly, geophysical anomaly, and geochemical anomaly, we can find the location of the required ore deposit; these areas are known as the favorable areas for prospecting. With more information on the geological anomaly, the area of the prospecting target will be gradually reduced, making it easy to locate the deposit. Therefore, the geological anomaly is the basis of mineral deposit prediction; it is effective in locating deposits by precisely identifying the geological anomaly. Therefore, it is important to identify more reasonable methods to locate the geological anomaly. To meet this challenge, various methods have been proposed and successfully applied with respect to the geological anomaly, such as the Three-Component Mineral Prediction theory ("as discussed by Zhao et al. [8]"), the quantitative prediction theory of geological anomaly ("as discussed by Pengda et al. [3]"), and singularity theories and methods for mineral deposit prediction ("as discussed by Cheng and Zhao [9]"). However, each method pertaining to the geological anomaly needs to meet the conditions of the algorithms when they identify the geological anomaly. In fact, not every algorithm satisfies the entire geological environment. Consequently, more algorithms related to the characteristics of the geological anomaly and those based on the environment are needed, which match the extraction criteria of the geological anomaly.

At the International Statistics Congress held in Seoul, Republic of Korea ("as discussed by Chen et al. [10]"), Pengda Zhao described the geological anomaly as an extreme value based on a mathematical foundation. For the geological background, he thought that an abnormal value was the geological anomaly, which directly infers that knowledge of the mathematical foundation of the geological anomaly is of extreme value. The extreme value analysis pertains to research on the random character in the process of quantification at a very large or small level and an estimate of the probability of an extreme event at the existing observational level, while the observation data of the geological anomaly are located in the tail end of the distribution. Therefore, the geological anomaly belongs to the EVT category. The extreme value theorem is a branch of statistics that studies the limiting distribution of the minimum and maximum value and evaluates the risk of extreme events ("as discussed by Allen et al. [11]"). In recent years, the EVT has been widely used in the fields of finance, insurance, floods, earthquakes, rainfall analysis, and so on ("as discussed by Chen and Lv [12]" and "as discussed elsewhere [12–14]"). Since the geological anomaly belongs to the EVT category, the EVT has been widely used in many fields, so we can learn from the experience of these types of applications and design the extreme value model of the geological anomaly that can effectively identify the geological anomaly. Does the EVT model of the geological anomaly really identify anomalies? This study was performed to verify the use of the model to identify anomalies in the Jiguanzui Cu-Au mining area. The results show that the model can effectively identify the geological anomaly region.

The rest of this paper is organized as follows. Section 2 studies the EVT, the method of selecting the threshold EVT is studied, and some parameters of the EVT are also discussed. Section 3 designs the EVT model of the geological anomaly and provides a new method to increase the accuracy with which the threshold can be selected. The feasibility of using the EVT model to identify the anomaly is discussed. Section 4 will demonstrate the application of the EVT model of the geological anomaly. Some conclusions are presented in Section 5.

2. The Study of the EVT

2.1. The Knowledge Related to the EVT. In the sample data, if the parent distribution or the sample size is not fully known, the parent distribution can be obtained from the asymptotic distribution of the extreme value of the sample. While the sample data are large, the largest or smallest value from a sample has a degradation problem. However, the extremal type theorem can effectively solve this problem ("as discussed by Vanem [15]"). The extremal type theorem is presented as follows.

If $x_1, x_2, \ldots, x_n$ is a sequence of independent random variables with a common distribution, parent distribution $F(x)$ is unknown. M_n is the largest value of the sample interval, and $H(x)$ is a nondegenerate distribution function. If there exists a sequence of constants $\{a_n\} > 0$ and $\{b_n\} \in R$,

$$\Pr\left(\frac{M_n - b_n}{a_n} \le x\right) \longrightarrow H(x). \tag{1}$$

$H(x)$ indicates a generalized extreme value distribution. Here, a_n is a scaling constant and b_n is a location constant. Then, this limiting distribution $H(x)$ after standardization $(M_n - b_n)/a_n$ must be one of the three following types:

$$H(x) = \begin{cases} 0, & x \le b \\ \exp\left\{-\left(\dfrac{x-b}{a}\right)^{-\alpha}\right\}, & x > b \end{cases}$$
$$\alpha > 0, \text{ (FRECHET)}$$
$$H(x) = \begin{cases} \exp\left\{-\left[-\left(\dfrac{x-b}{a}\right)^{-\alpha}\right]\right\}, & x \le b \\ 1, & x > b \end{cases} \tag{2}$$
$$\alpha < 0, \text{ (WEIBULL)}$$
$$H(x) = \exp\left\{-\exp\left[-\left(\frac{x-b}{a}\right)\right]\right\},$$
$$x \in R, \text{ (GUMBEL)}.$$

Here, α is a shape parameter, b is a location parameter, and a is a scale parameter.

2.2. The GPD Model. In the EVT, the block maxima method (BMM) is a traditional model ("as discussed by Rivas et al.

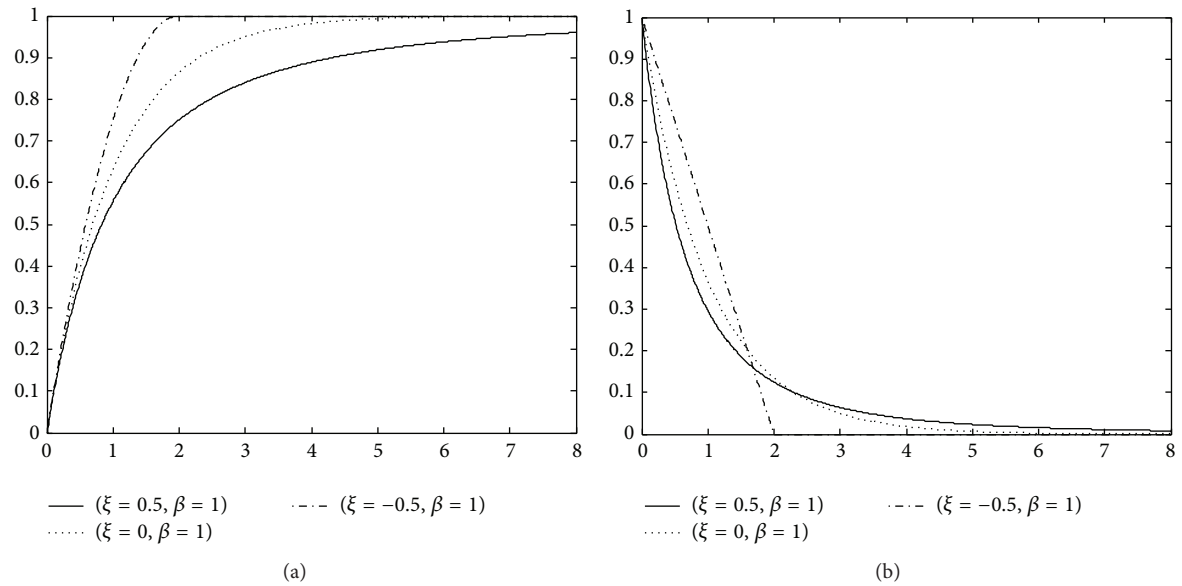

Figure 1: The standard GPD: (a) is the distribution function of the GPD and (b) is the density function of the GPD.

[16]"). The BMM divides the sample interval into several nonoverlapping cells in accordance with the time, the length, and so on. Then, there is an extreme sequence that is formed by selecting all the maximum values of each small interval; from the extreme sequence, the parent distribution can be obtained by distribution fitting of the extremal type theorem. However, the BMM model has a problem that some maximum values of intervals are greater than those of the other intervals; thus, the validity of the BMM model is not satisfactory. The defects can be solved by generalized Pareto distribution (GPD) ("as discussed by Ashkar and El Adlouni [17]"). The GPD is a fitting of the observed data, which is greater than a certain threshold.

Here, $x_1, x_2, \ldots, x_n$ is a sequence of independent random variables with a common distribution, and μ is a sufficiently high threshold. If there is positive number β, the excess distribution $(x_i - \mu,\ i = 1, 2, \ldots, n)$ can be expressed as

$$G_{\xi,\beta}(x) = \begin{cases} 1 - \left(1 + \xi \dfrac{x-\mu}{\beta}\right)^{-1/\xi}, & \xi \neq 0 \\ 1 - e^{-(x-\mu)/\beta}, & \xi = 0, \end{cases} \tag{3}$$

where ξ is a shape parameter and β is a scale parameter. If $\xi \geq 0$, $x \geq \mu$ and $\xi < 0$, $\mu \leq x \leq -\beta/\xi + \mu$. The sequence $(x_i,\ i = 1, 2, \ldots, n)$ obeys the GPD. The general formula of the GPD is given by

$$G_{\xi,\beta}(x) = \begin{cases} 1 - \left(1 + \dfrac{\xi}{\beta} x\right)^{-1/\xi}, & \xi \neq 0 \\ 1 - e^{-x/\beta}, & \xi = 0. \end{cases} \tag{4}$$

Here, if $\beta = 1$, the expression of the GPD is referred to as the standard form. If $\xi = -0.5$, 0.5, and 0, then the image of the standard distribution function and density distribution function of the GPD is as presented in Figure 1. From Figure 1(a), it is seen that the tail of the GPD thickens as the shape parameter increases. Figure 1(b) shows that the density function of the GPD decreases monotonically.

The GPD requires estimates of the parameters and threshold. The shape parameter ξ and scale parameter β of the GPD can be estimated by the maximum likelihood function ("as discussed by Castillo and Serra [18]"). Taking the derivative of (4), we can obtain the density function of the GPD:

$$f_{\xi,\beta}(x) = \frac{1}{\beta}\left(1 + \xi \frac{x}{\beta}\right)^{-1/\xi - 1}. \tag{5}$$

Taking natural logarithms of both sides of (5), we obtain the log likelihood function:

$$L(\xi, \beta : x) = -nLn\beta - \left(\frac{1}{\xi} + 1\right) \sum_{i=1}^{n} Ln\left(1 + \frac{\xi}{\beta} x_i\right). \tag{6}$$

Taking the partial derivative of ξ and β of (6), respectively, the likelihood equation is as follows:

$$\begin{aligned} n - \left(1 - \widehat{\xi}\right) \frac{\sum_{i=1}^{n} x_i}{\left[\widehat{\beta} + \widehat{\xi}(x_i)\right]} &= 0, \\ \sum_{i=1}^{n} \ln\left[1 + \frac{\widehat{\xi}(x_i)}{\widehat{\beta}}\right] - \sum_{i=1}^{n} \left\{\frac{x_i}{\left[\widehat{\beta} + \widehat{\xi}(x_i)\right]}\right\} &= 0. \end{aligned} \tag{7}$$

Thus, the maximum likelihood estimate value $\widehat{\xi}$ of the shape parameter ξ and the maximum likelihood estimate value $\widehat{\beta}$ of the scale parameter β can be obtained from (7). In addition, the shape parameter and scale parameter of the GPD can be estimated by the moment method; the estimation results obtained by the moment method are superior to those

obtained using the likelihood function ("as discussed by Ergün and Jun [19]"). The moment method is given by

$$\widehat{\xi} = \frac{\left[1 - \left(\bar{t}/\delta\right)^2\right]}{2}, \qquad \widehat{\beta} = \bar{t}\left(1 - \widehat{\xi}\right), \tag{8}$$

where $\bar{t}_i = x_i - \mu \geq 0$, $\bar{t}$ is the mean value of t_i, and δ is the standard deviation of t_i. In the GPD model, the threshold selection methods mainly concern the mean excess function (MEF) ("as discussed by Gencay and Selcuk [20]") and Hill plotting ("as discussed by J. H. T. Kim and J. Kim [21]"). If random variable X obeys the GPD, the MEF $E(\mu)$ is given by

$$E(\mu) = E(X - \mu \mid X > \mu) = \frac{(\beta + \mu\xi)}{(1 - \xi)}. \tag{9}$$

For the actual sample data, $E(\mu)$ can be calculated by the following:

$$E(\mu) = \frac{\sum_{i=1}^{n} (x_i - \mu)^+}{N_n}, \tag{10}$$

where n is the total number of sample data and N_n is the total number of sample data that exceed threshold μ. If $x_i \geq \mu$, $(x_i - \mu)^+ = x_i - \mu$ or $x_i < \mu$, $(x_i - \mu)^+ = 0$. Then, we can plot scatter diagram $(\mu, E(\mu))$. In the scatter diagram, there is sufficiently high threshold μ; when $x > \mu$, $E(\mu)$ is an approximate linear function.

3. Design the EVT Model of the Geological Anomaly

For the actual observational data $X = \{x_1, x_2, \ldots, x_n\}$ of the geological anomaly, the tail distribution of the geological observational data is called the geological anomaly. Therefore, if the data are higher than sufficiently high threshold μ in the sample data, we can model these data using the GPD. The parameters of the GPD can be estimated by the moment method or the likelihood function. Threshold μ can also be calculated using the MEF or Hill plotting. Thus, the designed EVT model of the geological anomaly is as follows.

Step 1 (conditional test). Before using the EVT model of the geological anomaly, the stationary and posttail of the sample data need to be tested. The common method of the conditional test is as follows: probability plot and quantile-quantile (Q-Q) plot ("as discussed by Feng et al. [22]"), augmented Dickey-Fuller (ADF) test ("as discussed by Lee and Chang [23]"), and so on.

Step 2 (estimate the parameters of the model). For the sample data, use the moment method or likelihood function to estimate shape parameter ξ and scale parameter β of the GPD.

Step 3 (determine the threshold). Select different thresholds μ from the sample data. Then, we can calculate the MEF of the sample data through scatter diagram $(\mu, E(\mu))$; there is sufficiently high threshold μ, when $x > \mu$, and $E(\mu)$ is an approximate linear function. Here, the value μ is called the threshold of the geological anomaly.

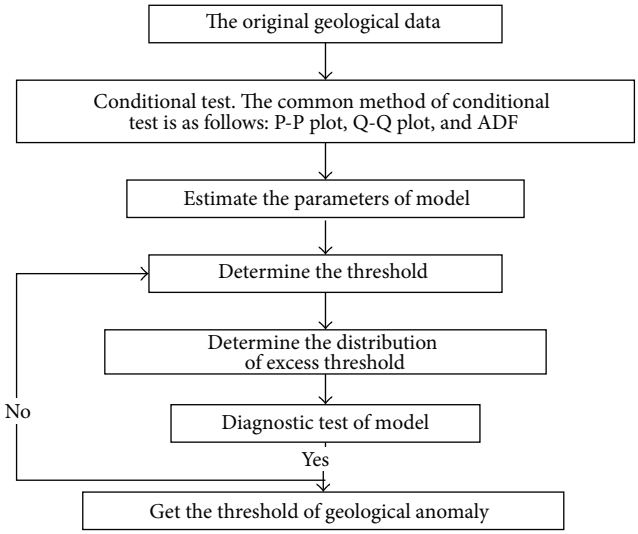

Figure 2: The chart of the algorithm.

Step 4 (determine the distribution of the excess threshold). After the threshold and parameters are determined, we insert the threshold and parameters into the GPD to obtain the distribution of the excess threshold; this distribution is called the abnormal probability distribution.

Step 5. After the distribution of excess threshold is determined, a diagnostic test can determine whether the threshold selection is rational. The diagnostic test of the model mainly tests the consistency between the theoretical distribution and the actual distribution, especially the fitting degree of the actual data and the model distribution. The methods we usually use are the Q-Q plot and probability plot. If the test effect is not satisfactory, repeat Step 3 and determine the new reasonable threshold. The chart of the EVT model of the geological anomaly is shown in Figure 2.

In this study, the determination of threshold μ in the EVT model is critical. If the selection of the threshold value is higher, the number of samples that exceed the threshold value is lower, and the parameters of the GPD are very sensitive to the high values of the observational data, which will cause errors in the parameter estimation. Conversely, the selection of a threshold value that is low will increase the number of observations, increasing the accuracy of the estimation of the parameters, but the excess data $x_i - \mu$ do not obey the GPD distribution. At present, there is no clear method to select the accuracy threshold. The MEF can be used to estimate the threshold with some defects, in which the selection of the threshold is usually an interval value and not an accurate constant. Therefore, this paper provides a new method to increase the accuracy with which the threshold can be selected. In the GPD, when the initial threshold value μ_0

Table 1: The basic statistics of Cu and Au.

Elements	Mean	Minimum	Maximum	Std. dev	CV	Skewness	Kurtosis
Cu	641.44	53.26	17202.77	727.65	1.13	7.38	106.96
Au	70.82	7.13	1877.97	0.25	0.82	8.42	154.93

is determined, the excess data $x_i - \mu_0$ approximately obey the GPD distribution. Regardless of any threshold μ ($\mu > \mu_0$), the shape parameter ξ and scale parameter β of the GPD should remain unchanged. Therefore, information can be obtained on the transformation relationship between $\beta(\mu)$ and threshold μ ($\mu > \mu_0$) from (3).

$$\beta(\mu) = \beta(\mu_0) + \xi(\mu - \mu_0). \tag{11}$$

Let $\beta^*(\mu) = \beta(\mu_0) + \xi(\mu - \mu_0)$; $\beta^*(\mu)$ is called the modified scale, and the values of $\beta^*(\mu)$ will not change when threshold μ changes. Therefore, when the interval threshold value is determined by MEF, the accuracy threshold can be estimated by $\beta^*(\mu)$. Estimating the threshold using $\beta^*(\mu)$ is detailed in Section 4.2.

In this paper, the EVT model of the geological anomaly takes full account of the characteristic of the geological anomaly distribution and the practical features of the EVT. Relative to the geological background value, the anomaly and extreme value can be used to describe the geological anomaly. The observations of the geological anomaly are located in the tail of the samples, which are related to the random characters in the process of quantification at the very large or small level and estimate the probability of the extreme event in the existing observation levels—these characteristics are also the contents of the EVT. The EVT is a branch of statistics that studies the limiting distribution of the minimum and maximum value and evaluates the risk of extreme events. Therefore, the mathematical foundation of the geological anomaly is described by the EVT. On the one hand, the EVT describes the characteristic of the geological anomaly distribution from the perspective of mathematics; the results from (3) show the distribution of the sample data, which is proved in (12). On the other hand, the EVT provides a quantitative and digital research method for predicting and evaluating the mineral resources, which is proved in Figure 10. Besides, this paper also discusses the methods of estimate parameters and the threshold of the EVT. Consequently, a mathematical statistical model is established for quantitative geological data and geology information where the data exceed the threshold of the sample in (12). Therefore, the ability of the EVT model to identify the geological anomaly is feasible.

4. The Model Application in Identifying the Geological Anomaly of the Jiguanzui Cu-Au Mining Area

In order to show the effect of identifying the anomaly using the EVT model with geological anomaly recognition, the model was applied to identify the anomaly in an actual mining area. The study data with Cu and Au originate from 26 exploration lines of the Jiguanzui Cu-Au mining area in Hubei, China. The count of the sample data with Cu and Au is 14309. The Jiguanzui Cu-Au mining deposit is the blind deposits at the lower part of the Quaternary overburden layer. Currently, I, II, III, and VII main ore body groups, 14 main ore bodies, and 105 small fragmentary ore bodies have been identified in the mining area. The main ore bodies of the Jiguanzui Cu-Au mining area are distributed in the 013 to 034 lines, which are 950 meters long, the width is 160–800 meters, the elevation ranges from −5 m to −1412 m deep extension, and the level projection area of the ore bodies is 0.58 square kilometers. The overall distribution of the ore bodies is northeast 30°, the trend of the ore bodies is northeast 15°–72°, and the local trend of the ore bodies is northwest. I, II, III, and VII ore bodies are arranged in the form of an echelon, in which the tendency is northwest and the local tendency is south. The main ore bodies occur in the fault basin at the edge of the northwestern rock body of the Tonglushan, near the contact zone of the dolomitic marble, the quartz monzonite diorite porphyry, and quartz diorite in the Lower Triassic Jialingjiang Formation, and near the different lithology and the echelon fracture of dolomitic marble. The pattern of the Jiguanzui Cu-Au mining deposit is shown in Figure 3.

4.1. The Condition Test of the Model

4.1.1. The Posttail Test of Sample Data. Firstly, this paper analyses the basic statistics of the Cu and Au elements, and the results are shown in Table 1. From Table 1, we can see that the skewness of the sample data is greater than zero, and the sample data are not normally distributed, that is, distributed to the right. By observing the coefficient of variation, it is seen that the coefficient of variation of Au is smaller than that of Cu, and the stability of Au is higher than that of Cu. Besides, the kurtosis of Cu and Au is greater than that of the normal distribution (of which the kurtosis value is 3), which results in a leptokurtic distribution for Cu and Au. Therefore, the distribution of Cu and Au is shown to be skewed to the right with leptokurtic characteristics. Secondly, in order to indicate the difference between the actual distribution and normal distribution, Q-Q plot can be used for the observation test (Figure 4). The distribution of Cu and Au is also shown to be skewed to the right with posttail characteristics.

4.1.2. The Stationary Test of the Sample Data. The stationary test mainly inspects the self-correlation of the geological data; the common methods of the stationary test are as follows: the augmented Dickey-Fuller (ADF) and sequence correlation analysis. Through the ADF, we can obtain the test results of the sample data (Table 2). The t-statistics of Cu and Au are −33.93498 and −13.19081, respectively, which are smaller than their own 1% significant level. Therefore, the sequences of Cu and Au do not have unit roots; they are stationary sequences. The results of the sequence correlation analysis are

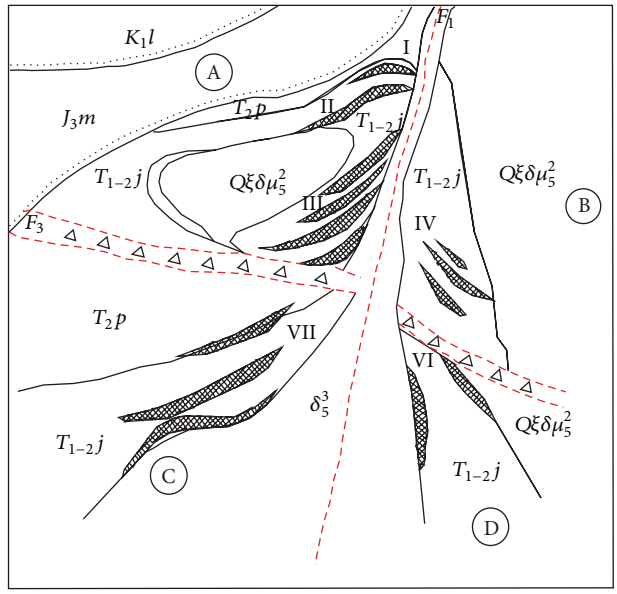

K_1l Volcaniclastic rocks of neighboring group

J_3m Breccia of Majiashan group

T_2p Pelitic siltstone of Puqi group

$T_{1-2}j$ Dolomitic marble of Lower Triassic Jialingjiang Formation

$Q\xi\delta\mu_5^2$ Quartz monzonite diorite porphyry

δ_5^3 Diorite

Fracture

Stratigraphic boundary

Unconformity boundary

Structural breccia

Ore bodies and numbers

Ⓐ The first metallogenic region

Ⓑ The second metallogenic region

Ⓒ The third metallogenic region

Ⓓ The fourth metallogenic region

Figure 3: The pattern of the Jiguanzui Cu-Au mining deposit.

Table 2: The ADF test of Cu and Au.

Elements	ADT (t-statistic)	Test critical values			Probability
		1% level	5% level	10% level	
Cu	−33.93498	−2.565127	−1.940847	−1.616685	0
Au	−13.19081	−2.565127	−1.940847	−1.616685	0

shown in Figure 5, where we can see that the autocorrelation coefficients (AC) and the partial autocorrelation coefficient (PAC) are not zero, and the significance of Q-states is high, so the uncorrelated hypothesis cannot be rejected. Therefore, the sequence of the geological data is a stationary time series.

Together, the results indicate that the data follow a stationary sequence, and the distributions of Cu and Au have posttail characteristics, indicating that they are abnormally distributed. Therefore, we can use the EVT model of the geological anomaly to identify the anomaly.

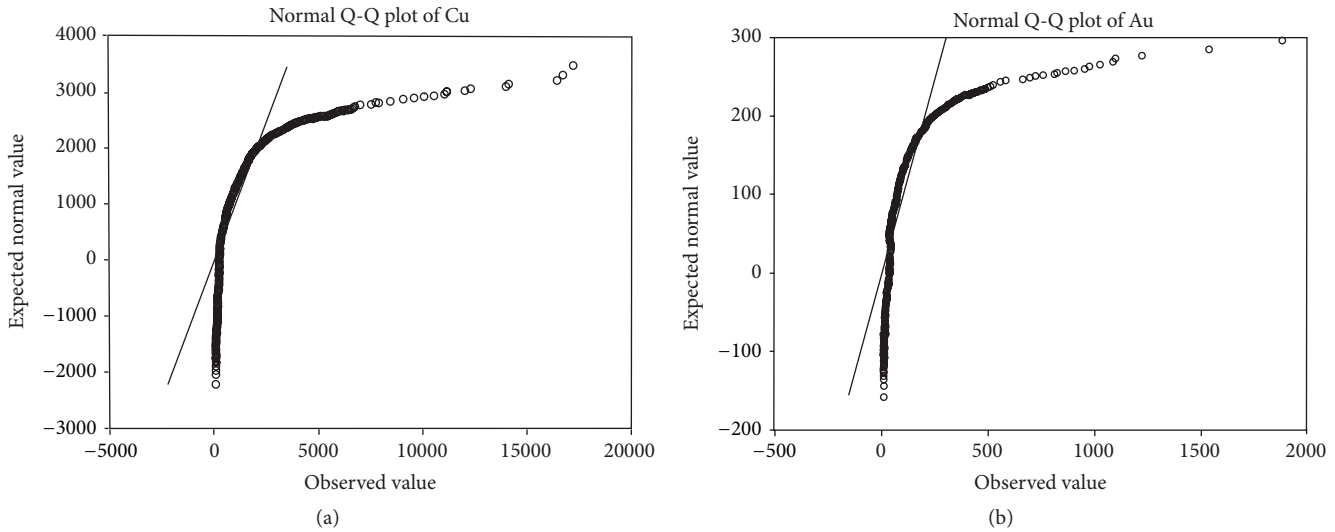

Figure 4: The posttail test of the sample data according to Q-Q plot. (a) is Q-Q plot test of Cu and (b) is Q-Q plot test of Au.

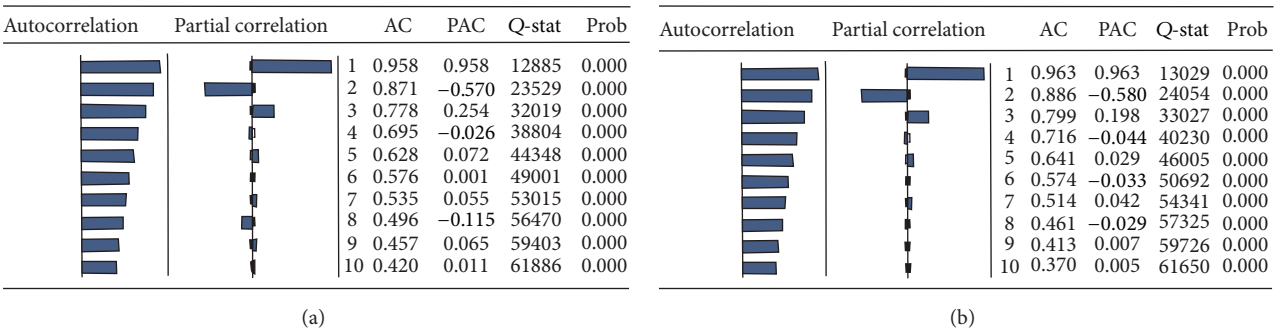

Figure 5: The sequence correlation analysis of the sample data. (a) is the sequence correlation analysis of Cu and (b) is the sequence correlation analysis of Au.

4.2. The Solution of the Model

4.2.1. Estimate the Parameters and Threshold. Through the EVT model of the geological anomaly, we can calculate the MEF of Cu and Au and plot the scatter diagram of the MEF (Figure 6). From Figure 6, it is seen that, in the interval [784.5406, 841.3659] with Cu and interval [72.1178, 85.1918] with Au, $E(\mu)$ for Cu and Au follows an approximately linear distribution. These intervals are selected as the threshold for Cu and Au. As the result of the threshold selection is subjective, modified scale $\beta^*(\mu)$ is used to estimate the accuracy threshold. Based on $\beta^*(\mu)$, if initial threshold value μ_0 is determined, regardless of any threshold μ ($\mu > \mu_0$), the shape parameter ξ and scale parameter β of GPD will not change. Uniformly selecting 50 threshold values from [784.5406, 841.3659] and [72.1178, 85.1918], respectively, we can obtain the transformation relations between $\beta^*(\mu)$, ξ, and the threshold μ ($\mu > \mu_0$) for Cu and Au using (3) and (11); see Figures 7 and 8. In order to ensure the accuracy of the EVT, the threshold selection is as large as possible in the permissible range of threshold estimation where the data show the stationary characteristic ("as discussed by Cao and Zhang [24]"). From Figures 7 and 8, it is seen that the threshold of Cu is 816.4006 and that of Au is 75.4736. After the thresholds are determined, the parameters of the EVT model of the geological anomaly can be estimated using the moment method, which reveals that the shape parameter of Cu is 0.3162 and that of Au is 0.3342; the scale parameter of Cu is 440.9216 and that of Au is 31.5699. Then, inserting the thresholds and parameters into the GPD, the distribution of the excess threshold of Cu and Au can be obtained by

$$F_{\mathrm{Cu}}(x) = 1 - \left(1 + \frac{0.3162}{440.9216}x\right)^{-1/0.3162},$$
$$F_{\mathrm{Au}}(x) = 1 - \left(1 + \frac{0.3342}{31.5699}x\right)^{-1/0.3342}. \quad (12)$$

The distribution of the excess threshold is called the abnormal probability distribution. In the mineral deposit prediction, information on the geological data can be described and expressed by the distribution of the excess threshold.

4.2.2. The Diagnostic Test of the Model and Identification of the Anomaly. The diagnostic test shows whether the

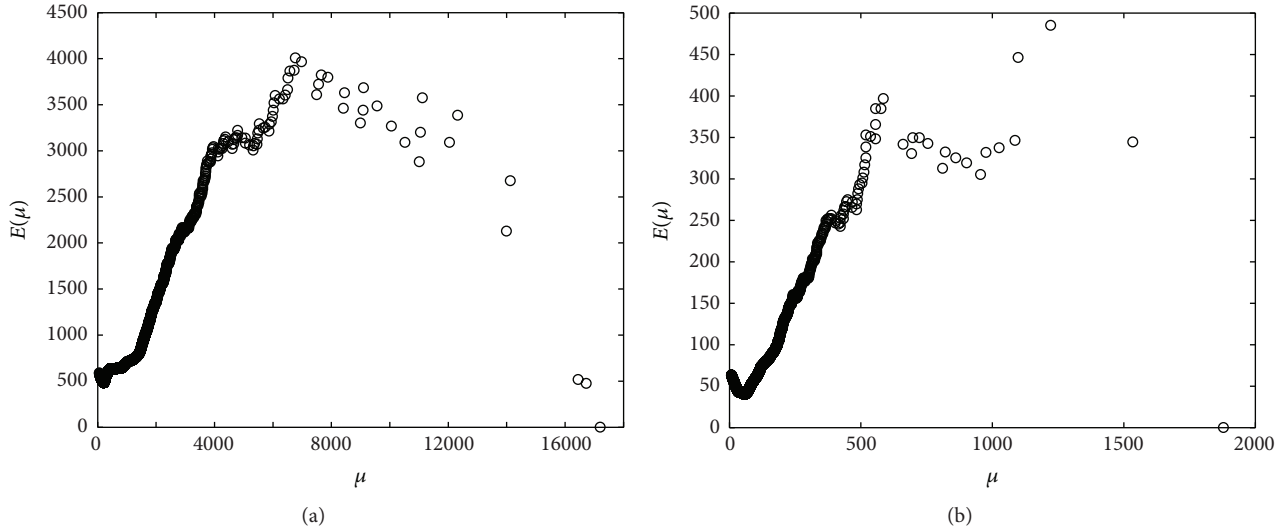

Figure 6: The scatter diagram of the MEF. (a) is the MEF of Cu and (b) is the MEF of Au.

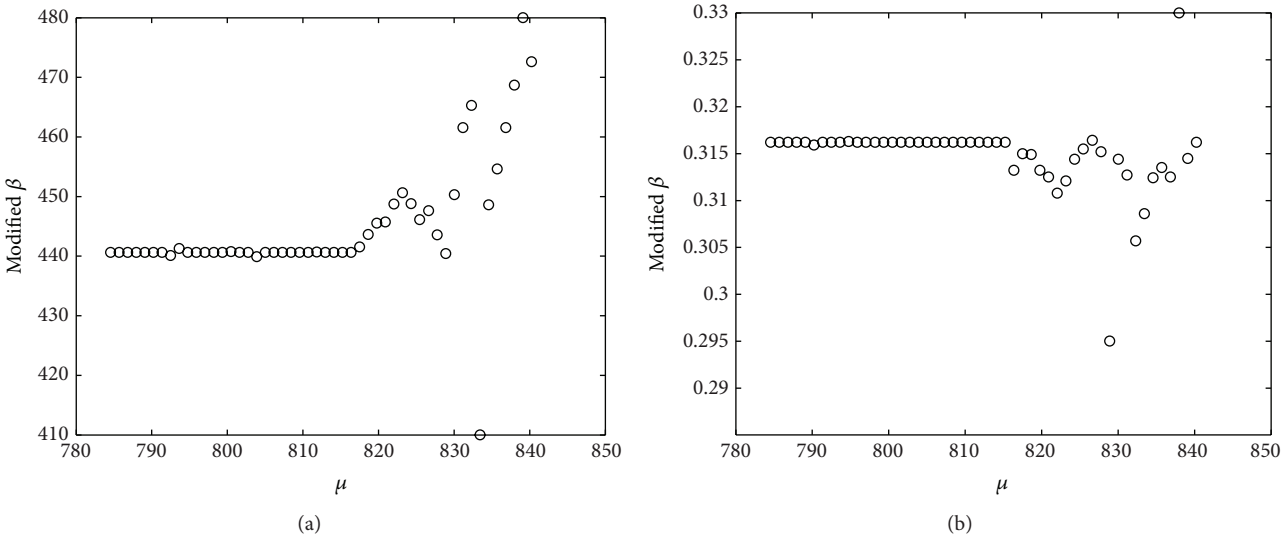

Figure 7: (a) and (b) show the relations between $\beta^*(\mu)$, ξ, and thresholds μ of Cu.

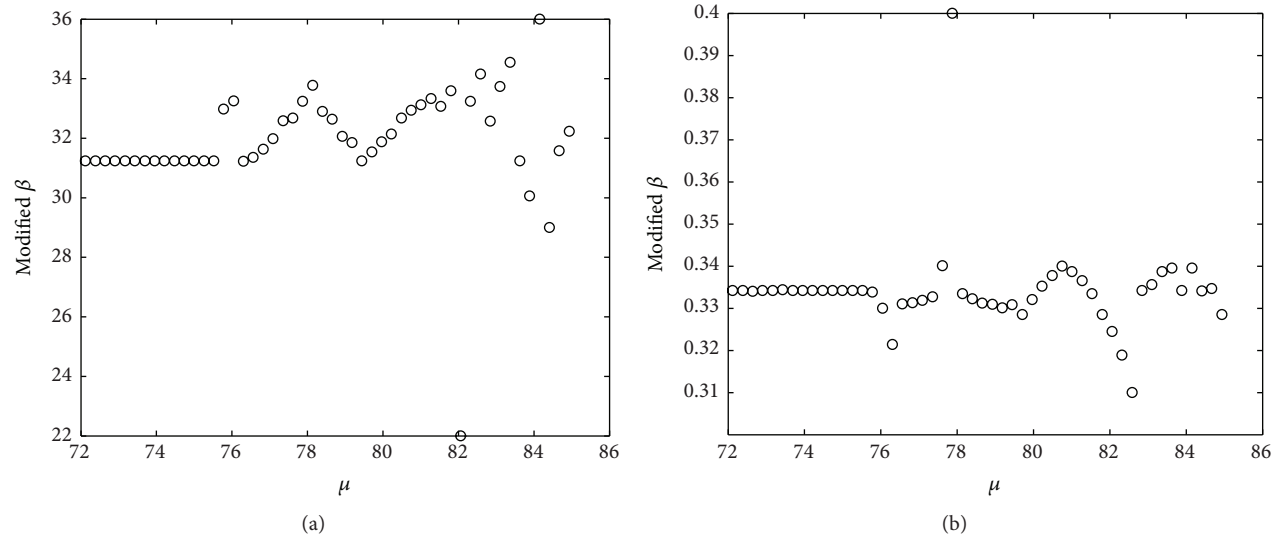

Figure 8: (a) and (b) show the relations between $\beta^*(\mu)$, ξ, and thresholds μ of Au.

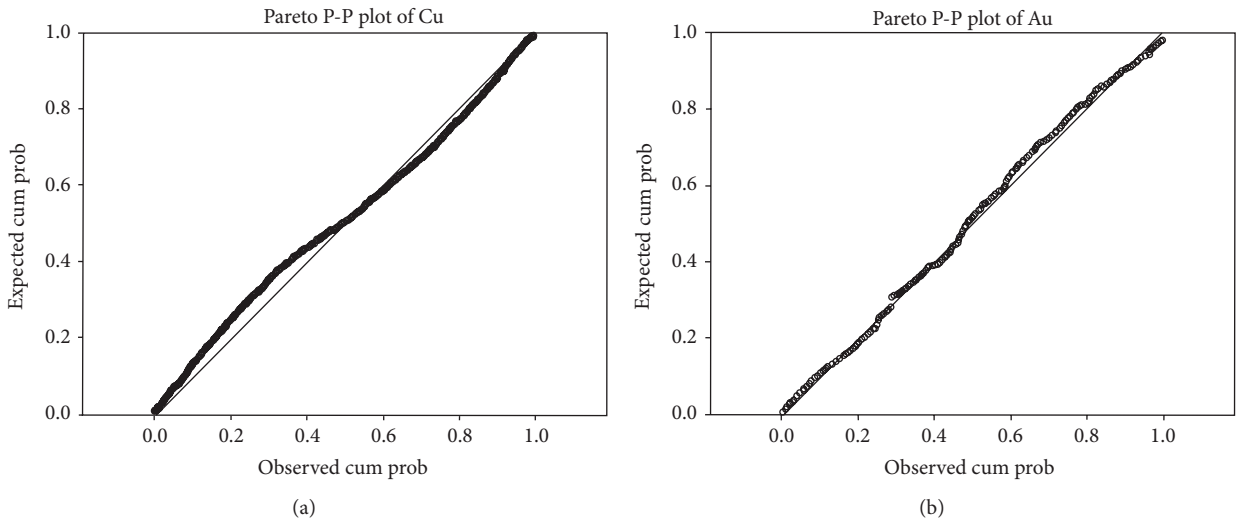

FIGURE 9: The GPD fitting of the sample data. (a) is the distribution fitting of Cu and (b) is the distribution fitting of Au.

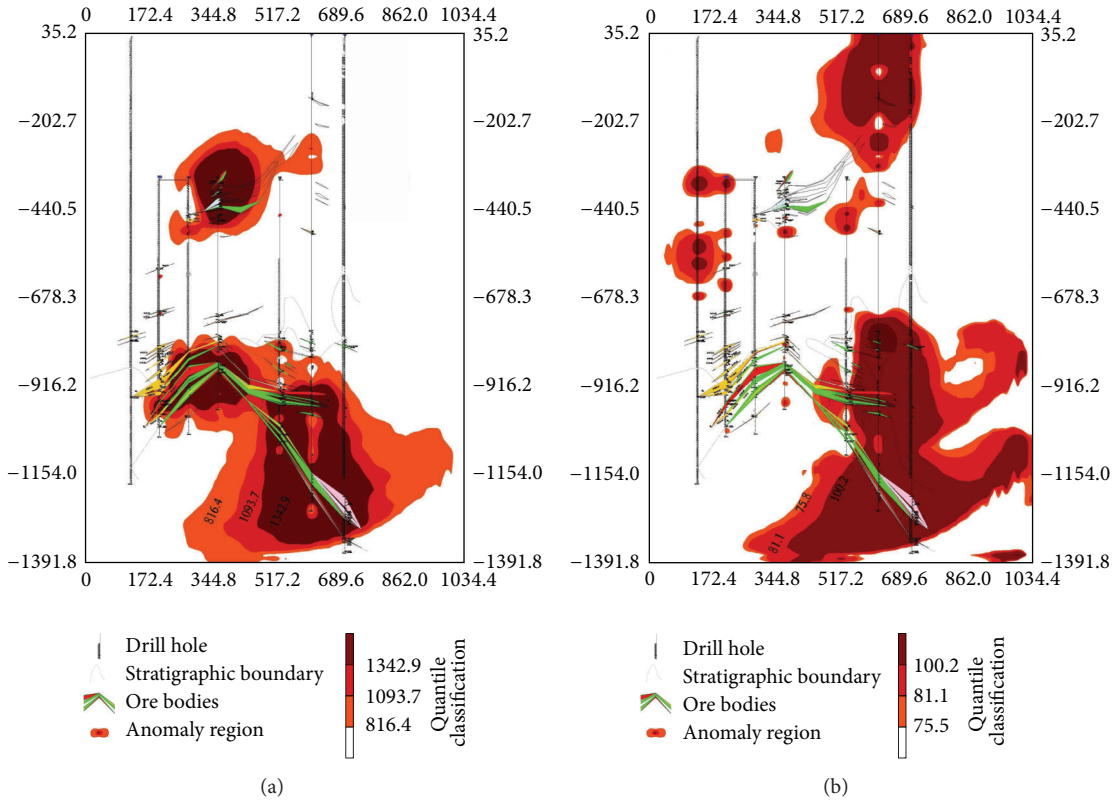

FIGURE 10: The identified anomaly region of Cu and Au. (a) is the anomaly region of Cu and (b) is the anomaly region of Au.

selection of the thresholds is reasonable. Fitting the excess threshold of the sample data using the GPD (Figure 9) indicates that the excess threshold of the sample data is in the vicinity of the line; the results show that the theoretical distribution and actual distribution of the sample data are consistent. Therefore, the threshold selection is reasonable. There are currently seven mining drill holes, that is, KZK10, KZK11, KZK23, KZK28, ZK02618, ZK02619, and ZK02620, and the exploitation ore bodies are mostly VII main ore body in the 26 exploration lines of the Cu-Au mining area. GIS technology is used to show the geological anomaly region with the selection of the thresholds (Figure 10). From Figure 10, it is seen that the anomaly region of Cu and Au is consistent with the range of ore bodies of the actual engineering exploration, which has a high indicating function with respect to ore prospecting. The results show

that the EVT model of the geological anomaly is good at mineral deposit prediction, and it has good prospecting significance.

5. Conclusion

In this study, the proposed EVT model of the geological anomaly was applied to identify geochemical anomalies associated with Cu and Au mineralization. The results of this study led to the following:

(1) The characteristics of the geological anomaly and the principle of EVT were studied; knowledge of the distribution of the EVT coincides with the distribution of the geological anomaly data. The designed EVT model of the geological anomaly takes full account of the characteristic of the geological anomaly and the practical features of the EVT. The threshold selection and parameter estimates of the model were determined.

(2) The proposed EVT model of the geological anomaly was successfully applied to identify the geological anomaly region in the Jiguanzui Cu-Au mining area. The results show that the anomaly threshold of Cu is 816.4006 and that of Au is 75.4736; the shape parameter of Cu is 0.3162 and that of Au is 0.3342; and the scale parameter of Cu is 440.9216 and that of the Au is 31.5699. The abnormal probability distribution was also determined. Testing the results of the model by fitting the excess threshold of the sample data showed that the results of the theoretical distribution and actual distribution of the sample data were consistent.

(3) The geological anomalies of Cu and Au predicted by the EVT model are consistent with the range of ore bodies of the actual engineering exploration. The EVT model has a high indicating function with respect to ore prospecting, and it is applicable for the exploration of mineral deposits.

Competing Interests

The authors declare that they have no competing interests.

Acknowledgments

This study was supported by the Geophysiochemistry Prospecting Institute of the Academy of Geological Science of China and the Program for the Core of High Spectrum of Primary Halo Geochemical Prospecting Project (no. 12120114002001), and the project of the special funds for universities was supported by the central government—the construction of discipline platform in management engineering theory and quantitative methods (no. 80000-14Z019002). The authors are grateful to the First Geological Brigade of the Hubei Geological Bureau for providing the data. They would also like to express their appreciation for the team members of the Key Laboratory of Mathematical Geology in Sichuan, China. They are grateful to Professor HongJun Liu at Chengdu University of Technology for providing constructive advice for this study. They also thank LetPub (http://www.letpub.com/) for its linguistic assistance during the preparation of this manuscript.

References

[1] A. Darehshiri, M. Panji, and A. R. Mokhtari, "Identifying geochemical anomalies associated with Cu mineralization in stream sediment samples in Gharachaman area, northwest of Iran," *Journal of African Earth Sciences*, vol. 110, pp. 92–99, 2015.

[2] X. Lu and P. Zhao, "Geologic anomaly analysis for space-time distribution of mineral deposits in the middle-lower Yangtze area, southeastern China," *Nonrenewable Resources*, vol. 17, no. 3, pp. 187–196, 1998.

[3] Z. Pengda, C. Qiuming, and X. Qinglin, "Quantitative prediction for deep mineral exploration," *Journal of China University of Geosciences*, vol. 19, no. 4, pp. 309–318, 2008.

[4] Q. Cheng, "Singularity theory and methods for mapping geochemical anomalies caused by buried sources and for predicting undiscovered mineral deposits in covered areas," *Journal of Geochemical Exploration*, vol. 122, pp. 55–70, 2012.

[5] A. P. Freedman and B. Parsons, "Geoid anomalies over two South Atlantic fracture zones," *Earth and Planetary Science Letters*, vol. 100, no. 1–3, pp. 18–41, 1990.

[6] P. Shen, Y. Shen, T. Liu, L. Meng, H. Dai, and Y. Yang, "Geochemical signature of porphyries in the Baogutu porphyry copper belt, western Junggar, NW China," *Gondwana Research*, vol. 16, no. 2, pp. 227–242, 2009.

[7] J. Zhao, S. Chen, and R. Zuo, "Identifying geochemical anomalies associated with Au–Cu mineralization using multifractal and artificial neural network models in the Ningqiang district, Shaanxi, China," *Journal of Geochemical Exploration*, vol. 164, pp. 54–64, 2016.

[8] P. Zhao, J. Chen, J. Chen, S. Zhang, and Y. Chen, "The 'three-component' digital prospecting method: a new approach for mineral resource quantitative prediction and assessment," *Natural Resources Research*, vol. 14, no. 4, pp. 295–303, 2005.

[9] Q. Cheng and P. Zhao, "Singularity theories and methods for characterizing mineralization processes and mapping geo-anomalies for mineral deposit prediction," *Geoscience Frontiers*, vol. 2, no. 1, pp. 67–79, 2011.

[10] Y. Chen, P. Zhao, J. Chen, and J. Liu, "Application of the geo-anomaly unit concept in quantitative delineation and assessment of gold ore targets in western Shandong uplift terrain, eastern China," *Natural Resources Research*, vol. 10, no. 1, pp. 35–49, 2001.

[11] D. E. Allen, A. K. Singh, and R. J. Powell, "Extreme market risk-an extreme value theory approach," *Mathematics and Computers in Simulation*, vol. 94, pp. 310–328, 2011.

[12] Q. Chen and X. Lv, "The extreme-value dependence between the crude oil price and Chinese stock markets," *International Review of Economics and Finance*, vol. 39, pp. 121–132, 2015.

[13] K. Whan, J. Zscheischler, R. Orth et al., "Impact of soil moisture on extreme maximum temperatures in Europe," *Weather and Climate Extremes*, vol. 9, pp. 57–67, 2015.

[14] D. Faranda, J. M. Freitas, P. Guiraud, and S. Vaienti, "Sampling local properties of attractors via extreme value theory," *Chaos, Solitons and Fractals*, vol. 74, pp. 55–66, 2015.

[15] E. Vanem, "Non-stationary extreme value models to account for trends and shifts in the extreme wave climate due to climate change," *Applied Ocean Research*, vol. 52, pp. 201–211, 2015.

[16] D. Rivas, F. Caleyo, A. Valor, and J. M. Hallen, "Extreme value analysis applied to pitting corrosion experiments in low carbon steel: comparison of block maxima and peak over threshold approaches," *Corrosion Science*, vol. 50, no. 11, pp. 3193–3204, 2008.

[17] F. Ashkar and S.-E. El Adlouni, "Adjusting for small-sample non-normality of design event estimators under a generalized Pareto distribution," *Journal of Hydrology*, vol. 530, pp. 384–391, 2015.

[18] J. D. Castillo and I. Serra, "Likelihood inference for generalized Pareto distribution," *Computational Statistics & Data Analysis*, vol. 83, pp. 116–128, 2015.

[19] A. T. Ergün and J. Jun, "Time-varying higher-order conditional moments and forecasting intraday VaR and Expected Shortfall," *The Quarterly Review of Economics and Finance*, vol. 50, no. 3, pp. 264–272, 2010.

[20] R. Gencay and F. Selcuk, "Extreme value theory and value-at-risk: relative performance in emerging markets," *International Journal of Forecasting*, vol. 20, pp. 287–303, 2004.

[21] J. H. T. Kim and J. Kim, "A parametric alternative to the Hill estimator for heavy-tailed distributions," *Journal of Banking & Finance*, vol. 54, pp. 60–71, 2015.

[22] Z.-H. Feng, Y.-M. Wei, and K. Wang, "Estimating risk for the carbon market via extreme value theory: an empirical analysis of the EU ETS," *Applied Energy*, vol. 99, pp. 97–108, 2012.

[23] C.-C. Lee and C.-P. Chang, "New evidence on the convergence of per capita carbon dioxide emissions from panel seemingly unrelated regressions augmented Dickey-Fuller tests," *Energy*, vol. 33, no. 9, pp. 1468–1475, 2008.

[24] G. Cao and M. Zhang, "Extreme values in the Chinese and American stock markets based on detrended fluctuation analysis," *Physica A: Statistical Mechanics and its Applications*, vol. 436, pp. 25–35, 2015.